Agrociencia

ANALYSIS OF THE SPATIAL ASSOCIATION OF FUMAGINA (*Capnodium* spp.) AND GREEN SCALE (*Coccus viridis*) IN COFFEE IN SULTEPEC, MEXICO

Alfredo **Ruiz-Orta**[1], Atenas **Tapia-Rodríguez**[2], Dulce Karen **Figueroa-Figueroa**[3], José Francisco **Ramírez-Dávila**[1*]

[1] Universidad Autónoma del Estado de México. Facultad de Ciencias Agrícolas. Carretera Toluca-Ixtlahuaca km 15, El Cerrillo Piedras Blancas S/N, entronque a El Cerrillo, Toluca, Estado de México, Mexico. C. P. 50200.
[2] Tecnológico de Estudios Superiores de Villa Guerrero. Carretera Federal Toluca-Ixtapan de la Sal km 64.5, Col. La Finca, Villa Guerrero, Estado de México, Mexico. C. P. 51763.
[3] Universidad Mexiquense del Bicentenario. Unidad de Estudios Superiores Coatepec Harinas 3. Ejido San Luis, El Reynoso, Coatepec Harinas, Estado de México, México. C. P. 51700.
* Author for correspondence: jframirezd@uaemex.mx

Citation: Ruiz-Orta A, Tapia-Rodríguez A, Figueroa-Figueroa DK, Ramírez-Dávila JF. 2023. Analysis of the spatial association of fumagina (*Capnodium* spp.) and green scale (*Coccus viridis*) in coffee in Sultepec, Mexico. **Agrociencia.** doi.org/ 10.47163/agrociencia.v57i7.2945

Editor in Chief:
Dr. Fernando C. Gómez Merino

Received: January 11, 2023.
Approved: June 15, 2023.
Published in Agrociencia: November 01, 2023.

ABSTRACT

The coffee crop (*Coffea arabica* L.) presents phytosanitary problems that can be economically significant if not properly managed, such as green scale (*Coccus viridis*) and fumagina (*Capnodium* spp.). Geostatistics is a tool that allows the producer to make optimal, timely, and accurate decisions for the integrated management of these problems. The objective of the research was to analyze the distribution and spatial association of fumagina and green scale in the coffee crop in Sultepec, State of Mexico, Mexico. During the first semester of 2022, random coffee plots were marked and geo-referenced for sampling. Several methods were used to obtain the spatial distribution of fumagina and green scale. The results showed fits of Gaussian, exponential, and mostly spherical geostatistical models, which represent an aggregate distribution and an association of these problems with each other. The estimation of the infested and infected area for both problems was obtained using the ordinary kriging method, revealing the presence of foci of infection and infestation. In plot three, it was identified that these are maintained and increase as the sampling progresses, finding a high degree of dependence and spatial stability. It is concluded that the populations of green scale and fumagina have an r value of 0.70, indicating a high association and correlation between them, which leads to a spatial distribution and possible management of targeted control of these phytosanitary problems and, in turn, sustainable management of the crop.

Keywords: Coffee culture, *Capnodium* spp., spatial correlation, spherical model.

INTRODUCTION

Coffee (*Coffea arabica* L.) represents one of Mexico's main agricultural export products, as well as one of the activities that generate employment in the states where it is grown. The cultivated surface of coffee is 710 897.41 ha, with a production value of MXN $5 210 614, therefore, its importance in the national economy is a fundamental factor

for the development of programs and projects that promote and support the coffee sector (CEDRSSA, 2019; SIAP, 2021); these programs cover not only economic aspects, but also production and marketing activities, as well as phytosanitary issues, which are promoted by governmental agencies in Mexico.

Coffee, like other crops of economic importance, is not free from phytosanitary problems; therefore, it is necessary to understand and identify pests and diseases in the crop in order to establish management programs that contribute to effective and timely decision-making in order to reduce economic losses for coffee growers. *Hyphotenemus hampei*, also known as the coffee berry borer, *Leucoptera coffeella* (the leaf miner), and scales such as *Selenaspidius articulatus* (articulated scale) and *Coccus viridis* (green scale), are among the pests affecting the coffee crop. In terms of diseases, those considered to have a high impact on the coffee crop are rust, iron spot, anthracnose, and rooster's eye; however, there have been reports of the presence of fumagina, as in the study conducted by González-Vega *et al*. (2007).

Fumagina in coffee is a disease caused by the saprophytic fungus *Capnodium* spp., which appears as black ash on sugary and sticky secretions produced by sucking insects such as aphids and scales, which feed on the sap of the plants and excrete this sweet and sugary secretion, commonly known as honeydew, on which some hymenopterous insects can feed. This fungus develops on branches, leaves, and fruits, covering the leaf area to the point of causing premature senescence and reducing growth as well as the photosynthetic capacity of the plant (González-Vega *et al*., 2007). The incidence of the disease becomes more prevalent in rainy seasons, and the number of diseased leaves increases considerably. Its presence is always caused by sucking insect attacks. The green coffee scale (*Coccus viridis*) is the most common species in coffee plantations less than two years old. Its foci cover the nerves of the leaves, as well as the petiole and the bark of branches and stems. Adults and nymphs feed on plant sap and excrete honeydew, which leads to fungal growth on the leaf surface and thus reduces photosynthesis. They also introduce toxins that cause plant weakening, leaf drop, and yield reduction if densities are high enough (Fernandes *et al*., 2011; Ong and Vandermeer, 2014; Gil-Palacio, 2020).

Several studies have reported the presence of fumagina not only in coffee but also in other important crops such as citrus, cocoa, soursop, guava, and mango, among others (Cárdenas-Murillo and Posada-Florez, 2001). Control alternatives for this problem have also been proposed; however, there are no studies in Mexico that show the spatial distribution of this disease and its relationship with the presence of insects such as green scale. In this regard, it is essential to recognize that in nature, organisms form aggregates or gradients in response to structural characteristics controlled by biotic and abiotic habitat variables, in order to contribute to a better understanding of the population dynamics of organisms and their relationship with the environment (Gómez-Campo *et al*., 2010).

Geostatistics comprises a set of tools and techniques used to analyze and predict the values of a variable that is distributed in space or time in a continuous manner; it

can also be defined as statistics related to geographic data, which is why it is also known as spatial statistics (Moral-García, 2004). Therefore, the objective of this work was to determine the distribution and spatial association of fumagina and green scale in the coffee crop in the municipality of Sultepec, State of Mexico, Mexico, as well as to promote targeted control management for these phytosanitary problems, which will allow for sustainable management of the crop in the study area.

MATERIALS AND METHODS

Study area

The research was conducted in the municipality of Sultepec in the State of Mexico (18° 52′ 00′′ N, 99° 57′ 00″ W, at an altitude of 2396 m) from January to June 2022; the municipality was selected because it has a representative coffee production of 60 ha for the state (SIAP, 2021).

Field work

Four plots of 0.5 ha were selected for coffee cultivation with a mixture of Caturra and Typica coffee varieties under conventional management with a polyculture system, with 40–60 % shade composed of parota, ash, orange, and lemon trees. Each plot was divided into 50 quadrats of 10 x 10 m, with four trees selected from each quadrat and georeferenced with a differential global positioning system (DGPS), for a total sample of 200 trees per plot. Each tree was sampled from four branches to determine the incidence (presence/absence) of green scale and 12 leaves from the same branches to detect the presence or absence of fumagina. From January to June 2022, sampling was done every fourteen days.

Geostatistical Analysis

To process the data obtained on disease incidence and scale in each of the samplings, Variowin 2.0 software (Primavara Verlag, New York, NY, USA) was used. Experimental semivariograms were obtained and fitted to theoretical models, which are usually spherical, exponential, and Gaussian, and then validated using the cross-validation method (Tapia-Rodríguez *et al*., 2020). Furthermore, the semivariogram parameters were determined: sill, range or reach, and nugget effect.

Level of spatial dependence

The level of spatial dependence of each phytosanitary problem was determined by dividing the nugget effect by the sill, with the result expressed as a percentage. The level of spatial dependence is considered high if it is less than 25 %, moderate if it is between 26 and 75 %, and low if it is greater than 76 % (Rivera-Martínez *et al*., 2020).

Kriging mapping and infected and infested surfaces

After adjusting the semivariograms, data interpolation was carried out using ordinary Kriging to visualize the spatial distribution patterns of the disease and the pathogen

over time; the estimates obtained were represented in the form of maps for each sampling, using the Surfer 16 program (Surfance Mapping System, Golden Software Inc., New York, NY, USA). Similarly, the infested surface of the microorganisms was calculated using the aforementioned program.

Spatial association

To determine the possible spatial association of the phytosanitary problems studied, a correlation analysis of means and a Tukey test at 0.05 % were performed using the Minitab 19 statistical software.

RESULTS AND DISCUSSION

In this study, the presence of green scale and fumagina was recorded in plots established with coffee crops in the municipality of Sultepec, State of Mexico, where 48 biweekly samplings were carried out, obtaining a total of 48 incidence maps and 48 semivariograms adjusted to theoretical models for green scale and the same amount for fumagina. For the green scale insect, most of the samplings were adjusted to spherical models (Table 1), except in plot one, where the spatial distribution was adjusted to exponential models in most of the months, presenting spherical models only in the second sampling in March and both samplings in May.

Table 1. Models and parameter values obtained for each semivariogram of the respective samplings of green scales (*Coccus viridis*) (January to June 2022).

Sampling	Mean	Variance	Model	Nugget	Sill	Range	Nugget/ sill	Spatial dependence
				Plot 1				
January 1	5.33	485.16	Exponential	0	431.2	12	0	high
January 2	5.50	498.84	Exponential	0	415	13.6	0	high
February 1	5.71	517.37	Exponential	0	436.8	11.6	0	high
February 2	5.93	543.99	Exponential	0	473	13.6	0	high
March 1	8.19	1188.07	Exponential	0	996	13.2	0	high
March 2	9.29	1251.01	Spherical	0	1040	9.6	0	high
April 1	9.76	1302.68	Exponential	0	1144	8.4	0	high
April 2	9.88	1271.01	Exponential	0	1078.96	9.99	0	high
May 1	9.83	1216.23	Spherical	0	974.95	10.08	0	high
May 2	11.60	1400.45	Spherical	0	1105.95	12	0	high
June 1	12.43	1565.32	Exponential	0	1344	13.19	0	high
June 2	13.48	1748.37	Exponential	0	1422	14	0	high
				Plot 2				
January 1	2.59	75.38	Spherical	0	60.8	7.6	0	high
January 2	3.12	128.32	Gaussian	0	101.4	6	0	high
February 1	2.37	107.89	Spherical	0	93.5	8.4	0	high
February 2	3.79	1096.71	Spherical	0	160	8.4	0	high
March 1	2.51	114.11	Spherical	0	102	6.8	0	high
March 2	5.98	1139.53	Spherical	0	576	8.4	0	high

Table 1. Continue.

Sampling	Mean	Variance	Model	Nugget	Sill	Range	Nugget/ sill	Spatial dependence
April 1	5.93	1135.89	Spherical	0	660	8.4	0	high
April 2	6.62	1149.91	Gaussian	0	672	6.4	0	high
May 1	6.97	1167.30	Spherical	0	684	9.2	0	high
May 2	7.1	1027.65	Spherical	0	605	8	0	high
June 1	6.65	599.22	Spherical	0	384	8.8	0	high
June 2	7.05	658.25	Spherical	0	415.8	7.6	0	high
				Plot 3				
January 1	8.88	899.50	Spherical	0	774	6.8	0	high
January 2	9.77	1052.51	Spherical	0	913	8	0	high
February 1	12.95	1614.38	Spherical	0	1360	6.39	0	high
February 2	10.66	1545.03	Spherical	0	1344	8	0	high
March 1	10.64	1440.28	Exponential	0	1155	9.2	0	high
March 2	12.46	1569.78	Spherical	0	1264	6.8	0	high
April 1	11.79	1329.11	Spherical	0	1148	7.6	0	high
April 2	11.62	1198.67	Spherical	0	1080	6.8	0	high
May 1	11.87	1223.87	Spherical	0	1092	7.2	0	high
May 2	12.29	1230.37	Spherical	0	1105	7.2	0	high
June 1	12.16	1229.24	Spherical	0	1092	7.2	0	high
June 2	12.67	1283.52	Spherical	0	1092	7.2	0	high
				Plot 4				
January 1	7.92	1293.12	Spherical	0	1597	3.07	0	high
January 2	7.97	1292.53	Gaussian	0	1743	4.05	0	high
February 1	8.39	1428.15	Exponential	0	1560	6.3	0	high
February 2	8.1	1398.45	Exponential	0	915	3.36	0	high
March 1	10.34	1985.66	Spherical	0	1633	4.32	0	high
March 2	10.94	1854.33	Spherical	0	1428	7.6	0	high
April 1	11.57	2224.56	Gaussian	0	1245	5.2	0	high
April 2	9.08	1685.28	Spherical	0	1595	7.6	0	high
May 1	9.70	2026.74	Gaussian	0	896	6	0	high
May 2	9.50	1827.48	Spherical	0	806	4.32	0	high
June 1	9.08	1538.16	Gaussian	0	1368	6.3	0	high
June 2	8.86	1456.86	Spherical	0	1232	6.3	0	high

In plots two and three, the spatial distribution of green was associated with spherical-type patterns for the majority of the sampling months. Biologically, the spherical model adjustment represents that the insect was identified more in certain points than in others, which means that there are defined pest aggregation centers that remain stable in the plots, presenting a strong relationship between them, which agrees with the work done by Martínez-Martínez *et al.* (2021) for armored scale (*Hemiberlesia lataniae*). It is interesting to note that for plot four, the insect distribution was adjusted not only to spherical models but also to Gaussian and exponential models, showing spherical models in the sampling of January, March, and in the second sampling of April, May, and June. For the rest of the months, the resulting models were exponential in February and Gaussian in the first sampling of January, April, May, and June.

Rivera-Martínez *et al.* (2020) mentioned that the adjustment to the Gaussian model indicates a continuous aggregation behavior within the study area, indicating that the pest will tend to spread, while Martínez-Martínez *et al*. (2021) mentioned that the exponential model, for armed scale in avocado, refers to an aggregate distribution of irregular limits within the plot and that it presents an accelerated growth that later stabilizes. Regarding the geostatistical analysis, it can be observed that a high level of spatial dependence was found on all sampling dates, which indicates the existence of a high spatial relationship between each sampling point.

Among the parameters that define the characteristics of the adjusted models is the range, whose value in meters is indicative of the level of spatial association that exists between the values of incidence. In this case, the range values for green scale in plot one were 8.4 m as a minimum and 13.6 m as a maximum, while for plot two, these values were 6 and 9.2 m. The maximum range values in plots three and four were 9.2 and 7.6 m, respectively, with minimum values of 6.39 and 3.07 m. This range distance indicates the extent to which the sampled data is spatially dependent. Beyond the maximum value of the distance, it was identified that there is such dependence between the population density of the phytosanitary problems in the sampled plots (Ramírez-Dávila, 2012).

As for the sill parameter, the lowest values for the green scale samples were mostly associated with Gaussian-type models, while the highest values were presented by spherical models in the four study plots. Biologically, this parameter associated with the range indicates the point where there is a greater spatial relationship between organisms, as mentioned by Ramírez-Dávila (2012).

The nugget effect is also shown, which for all sampling dates presented values of zero (Table 1), indicating that the sampling scale was appropriate for monitoring the green scale. This is in agreement with Oliver and Webster (1998), who suggest that having zero values for the nugget not only demonstrates that the sampling error was minimal, but also indicates that the adjusted models provide 98 % reliability. In the case of fumagina, the spatial distribution was adjusted to exponential, spherical, and Gaussian models in the four plots sampled; however, there is a certain predominance of spherical models, especially in the samples taken in plot three (Table 2).

The minimum range value for plot one was 4.07 m, associated with a Gaussian model in the second sampling in March and May, respectively, while the maximum range in this plot was 9.03 m, associated with an exponential model for the first sampling in April. For plot two, the maximum value was 5.1 m and the minimum was 3.14 m, with the latter associated with a Gaussian model and the maximum value again associated with an exponential model. Plots three and four had maximum fumagina distribution range values of 5.16 and 3.29 m, respectively, with minimum values of 3.52 and 2.42 m. The range values found express that the validity of the adjusted models extends to reasonable distances in terms of explaining the aggregation phenomenon of the disease (Solares-Alonso *et al.*, 2011), applying in the same way for green scale in this study.

Table 2. Models and parameter values obtained for each semivariogram of the respective fumagina (*Capnodium* spp.) sampling (January to June 2022).

Sampling	Mean	Variance	Model	Nugget	Sill	Range	Nugget/ sill	Spatial dependence
				Plot 1				
January 1	2.32	31.22	Spherical	0	66.64	5.1	0	high
January 2	2.40	33.92	Spherical	0	65.7	5.78	0	high
February 1	2.54	39.64	Gaussian	0	73.91	4.2	0	high
February 2	2.62	44.03	Spherical	0	70.17	6.01	0	high
March 1	3.27	49.35	Gaussian	0	58.22	4.07	0	high
March 2	4.01	72.40	Spherical	0	51	5.78	0	high
April 1	3.86	70.61	Exponential	0	41.36	9.03	0	high
April 2	3.67	59.54	Spherical	0	69.91	5.59	0	high
May 1	4.005	67.89	Gaussian	0	26.24	4.41	0	high
May 2	4.16	76.07	Gaussian	0	28.56	4.07	0	high
June 1	4.42	84.10	Spherical	0	48.5	5.77	0	high
June 2	4.61	87.19	Gaussian	0	33.6	4.42	0	high
				Plot 2				
January 1	2.07	25.36	Spherical	0	56.32	4.9	0	high
January 2	2.16	28.41	Spherical	0	26.35	4.55	0	high
February 1	2.23	31.07	Gaussian	0	54.28	4.08	0	high
February 2	2.35	37.35	Spherical	0	13.76	4.2	0	high
March 1	1.33	3.67	Gaussian	0	38.70	4.55	0	high
March 2	1.81	15.29	Spherical	0	41.6	4.2	0	high
April 1	2.77	49.06	Gaussian	0	62.09	4.19	0	high
April 2	2.97	51.45	Exponential	0	30.78	4.55	0	high
May 1	3.50	63.32	Gaussian	0	20.8	4.08	0	high
May 2	3.77	68.65	Exponential	0	23.49	5.1	0	high
June 1	3.76	59.19	Gaussian	0	2.51	3.14	0	high
June 2	4.11	70.96	Gaussian	0	58.22	4.55	0	high
				Plot 3				
January 1	2.33	30.70	Spherical	0	56.07	5.09	0	high
January 2	2.48	35.55	Spherical	0	58.5	5.1	0	high
February 1	2.60	40.14	Spherical	0	52.16	5.04	0	high
February 2	2.68	46.32	Spherical	0	42.29	4.16	0	high
March 1	3.46	63.27	Spherical	0	52.92	3.84	0	high
March 2	3.58	64.77	Gaussian	0	51.33	4.16	0	high
April 1	3.53	62.47	Spherical	0	63.95	5.10	0	high
April 2	3.66	58.54	Gaussian	0	72.09	4.42	0	high
May 1	4.24	78.51	Exponential	0	27.9	5.11	0	high
May 2	4.3	77.58	Gaussian	0	27.9	3.52	0	high
June 1	4.39	80.67	Spherical	0	36.8	4.47	0	high
June 2	4.65	88.90	Exponential	0	69.51	4.48	0	high
				Plot 4				
January 1	2.11	20.17	Spherical	0	24.32	3.29	0	high
January 2	2.27	23.78	Spherical	0	45.36	2.85	0	high
February 1	2.38	27.09	Gaussian	0	54.81	2.42	0	high
February 2	2.5	31.61	Gaussian	0	30.78	2.64	0	high
March 1	2.83	37.41	Exponential	0	64.3	2.71	0	high

Table 2. Continue

Sampling	Mean	Variance	Model	Nugget	Sill	Range	Nugget/ sill	Spatial dependence
March 2	3.13	46.66	Exponential	0	66.5	2.64	0	high
April 1	3.6	69.59	Gaussian	0	57.6	2.42	0	high
April 2	3.68	70.05	Spherical	0	51.85	2.63	0	high
May 1	3.57	63.19	Gaussian	0	16.38	2.64	0	high
May 2	3.55	60.88	Gaussian	0	20.16	2.64	0	high
June 1	3.39	53.29	Spherical	0	21.33	3.08	0	high
June 2	3.72	63.71	Spherical	0	41.83	3.08	0	high

The values for the sill were 2.51 as a minimum in plot two and 73.91 in plot one; likewise, the nugget effect also presented, as for green scale, values of zero, indicating a minimum sampling error. The creation of semivariogram-based density maps is another important tool in the spatial analysis of agricultural pests and diseases. For the 48 samplings in this study, infestation and infection maps were created, which graphically depict the behavior of the pest and disease analyzed within the study area. These maps were obtained through the ordinary kriging method, to estimate the percentages of infested and infected areas, as well as the values associated with unsampled points.

Density maps have been useful tools in studies of pest and disease behavior in agricultural crops, such as the study conducted by Quiñones-Valdez *et al*. (2015), who carried out spatial distribution and mapping of thrips infestations in gladiolus; as well as that reported by Jiménez-Carrillo *et al.* (2013) in the cultivation of husk tomato, who determined that the pests formed aggregation centers.

In the present work, through the maps generated, the presence of at least four green scale aggregation centers was detected in plot one (Figure 1), which coincided with a high population density and were maintained over time during the months of sampling. The green scale aggregation centers correspond to the aggregation centers formed by fumagina, although in this case, the disease has about six aggregation centers that remained stable during most of the sampling.

For plot two (Figure 2), the green scale showed well-defined infestation foci during the first five samples, but the foci dissipated in the remaining samples, though they remained constant as population density in the aggregation centers increased. Likewise, in the particular case of fumagina, more than six aggregation centers were observed, which were not only maintained over time, but also increased after the first sampling in April, reaching a maximum of twelve well-defined aggregation centers.

The presence of three aggregation centers formed by the presence of green scale is clearly observed in plot 3 (Figure 3), and this behavior is maintained throughout the twelve samplings carried out. In the case of fumagina, the centers of aggregation are

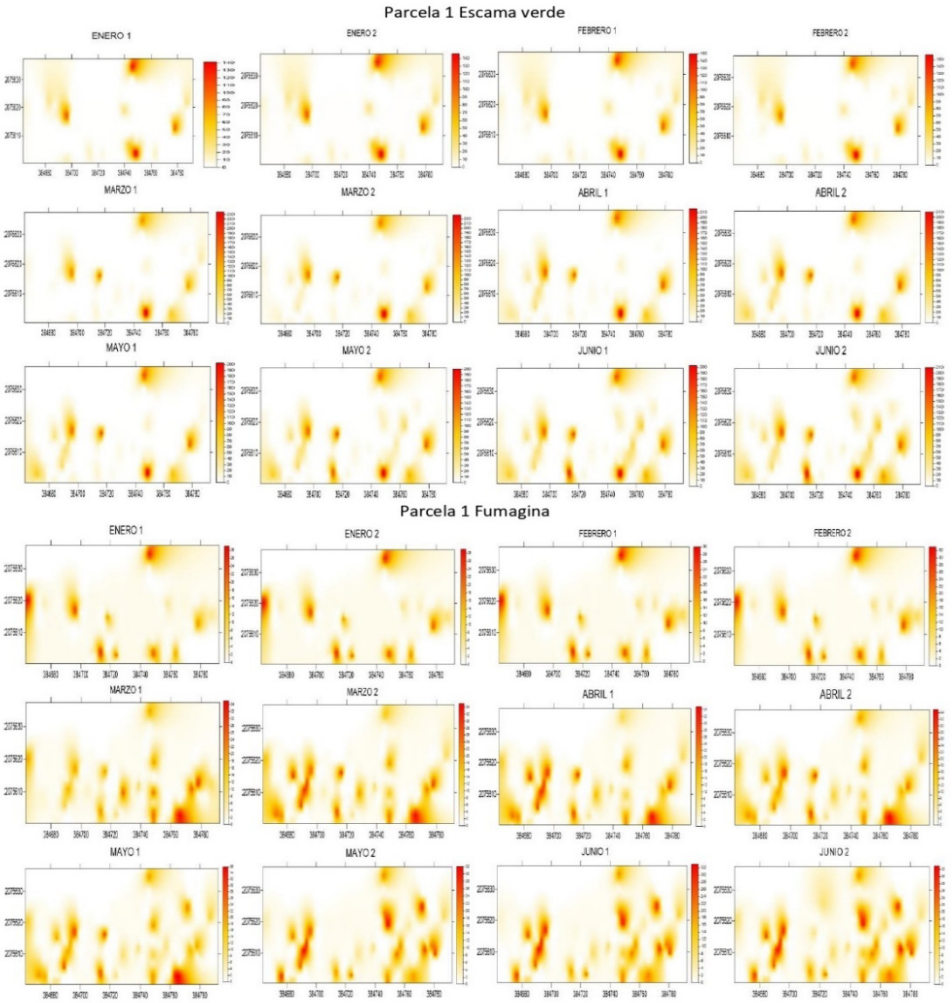

Figure 1. Biweekly maps of density and spatial distribution of green scale (*Coccus viridis*) and fumagina (*Capnodium* spp.) for Plot 1 (January to June 2022). *1: First two weeks of the month; 2: second two weeks of the month.

maintained and grow as the disease is sampled, indicating not only stability but also corroborating the level of spatial dependence.

In the case of plot 4 (Figure 4), the presence of two aggregation centers was identified, which were maintained throughout the sampling period. On the other hand, fumagina demonstrated the presence of more than four aggregation centers from the start of the sampling, as well as the presence of the disease in 80 % of the sampling area.

Density maps can be very useful in an integrated pest and disease management program for coffee cultivation, since it is possible to direct control measures towards the specific points of infestation and infection shown in the respective map, as

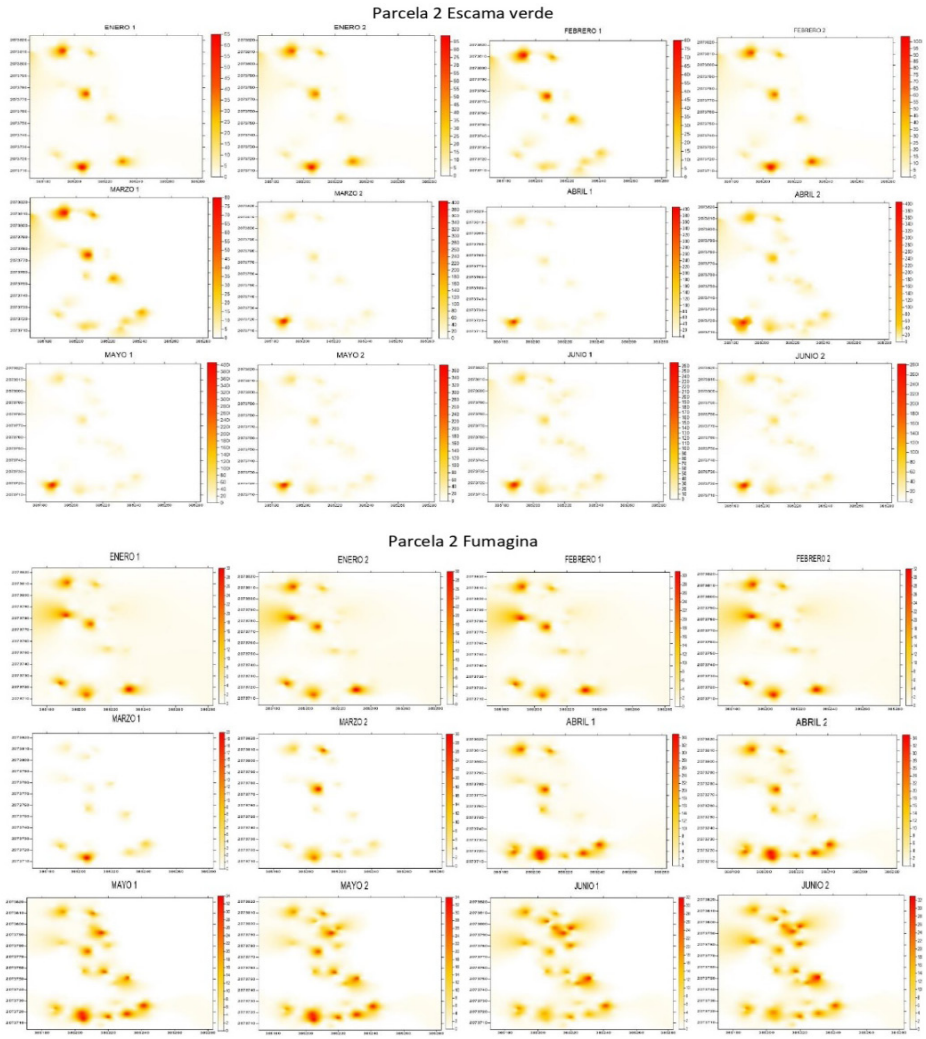

Figure 2. Biweekly maps of density and spatial distribution of green scale (*Coccus viridis*) and fumagina (*Capnodium* spp.) for Plot 2 (January to June 2022). *1: First two weeks of the month; 2: second two weeks of the month.

reported by Moral-García (2004). For a better spatial analysis of pests and diseases in agricultural crops, it is important to determine the level of infestation and infection in the study areas, which allows us to know exactly how the area is and thus determine appropriate control and prevention actions.

In the present work, the infested area was determined for the 48 green scale samples (Table 3), finding infestation percentages higher than 70 % in most of the samples taken. Works such as Esquivel-Higuera and Jasso-García (2015) also show pest

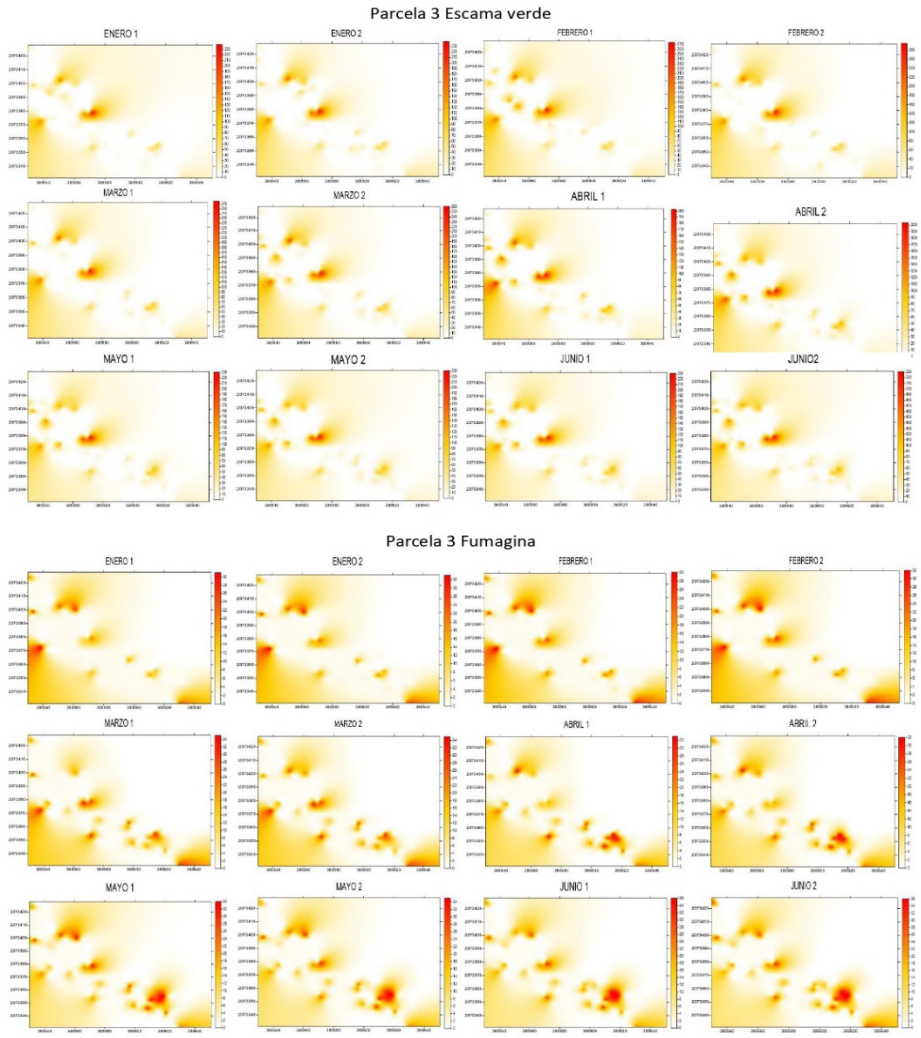

Figure 3. Biweekly maps of density and spatial distribution of green scale and fumagina for Plot 3 (January to June 2022). *1: First two weeks of the month; 2: second two weeks of the month.

Table 3. Correlation of means and Tukey's test between populations of green scale (*Coccus viridis*) and fumagina (*Capnodium* spp.).

Plot	Correlation (r)	*p* value
1	0.977	0.000
2	0.807	0.002
3	0.649	0.022
4	0.57	0.050
General value	0.706	0.000

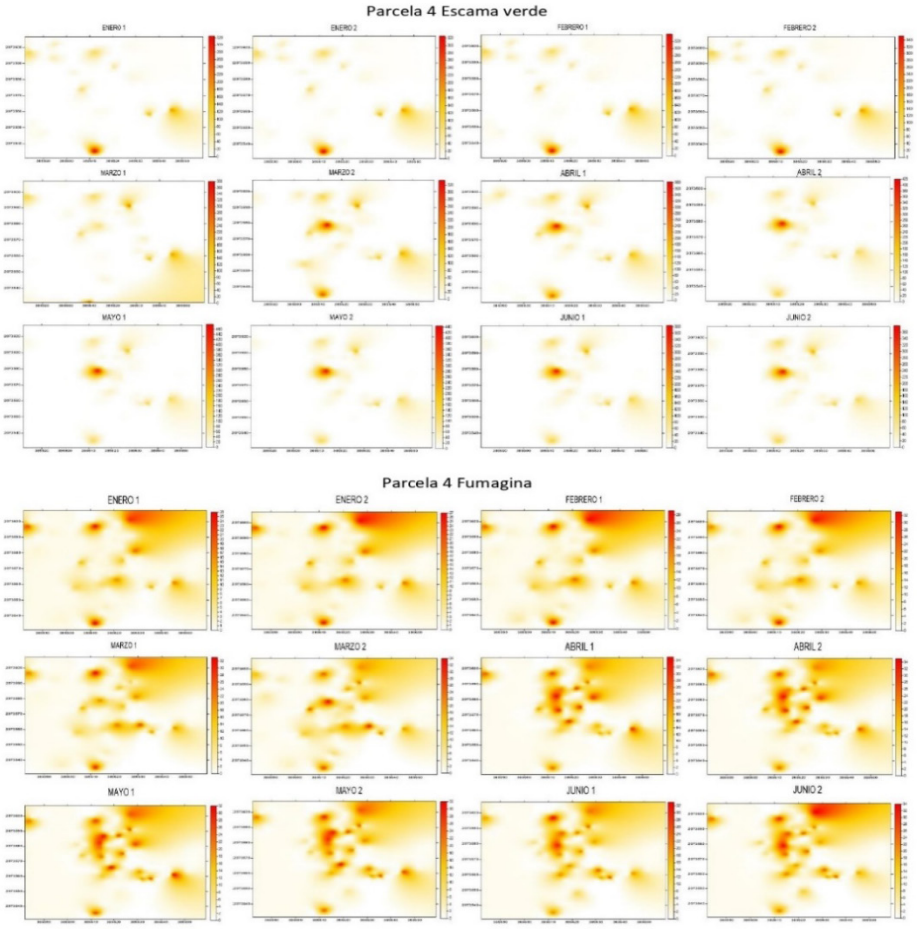

Figure 4. Biweekly maps of density and spatial distribution of green scale (*Coccus viridis*) and fumagina (*Capnodium* spp.) for Plot 4 (January to June 2022). *1: First two weeks of the month; 2: second two weeks of the month.

infestation percentages in plots where there is no relationship between the percentage and the density of infestation.

The months with the highest percentages of infestation are May and June in plot three, where infestation exceeds 70 %. In the remaining plots, the percentages remained between 59 and 70 %. This is consistent with the higher and lower densities of population fluctuation of the pest within the study area. It should be noted that the percentage of infestation is not directly related to the population density of the pest, as very high levels of infestation can occur at low densities that do not exceed the pest's economic threshold. In the case of fumagina, the infection percentages exceed 80 % for plot four, while for plots one, two, and three, the minimum percentage is 65 % and the maximum is 75 %.

The correlation analysis of means to determine the possible spatial association of the phytosanitary problems studied yielded a r value of 0.97 for plot one, 0.80 for plot two, 0.64 for plot three, and 0.57 for plot four (Table 3). The overall value of r for the four plots was 0.70, implying that there is a strong relationship between both phytosanitary problems. This coincides with Martínez-Ortega *et al.* (2009), who state that values close to 1 present a strong positive correlation, as well as that mentioned by Gil-Palacio (2020) and González-Vega *et al.* (2007), who indicate that the presence of *Capnodium* spp. is directly caused by *C. viridis*.

The spatial behavior of pests and diseases suggests that they can be managed, and therefore this is of great help in the use of control methods directed towards the centers of aggregation, thus avoiding widespread applications and having significant economic savings in the application of chemicals or alternative methods, which leads to a lower local, national, and international environmental impact (Schotzko and O'keeffe, 1989; Bautista *et al.*, 2013; Rivera-Martínez *et al.*, 2022).

CONCLUSIONS

The phytosanitary problems of green scale caused by the insect (*Coccus viridis* L.) and fumagina (*Capnodium* spp.) mostly presented a spatial distribution that adjusted to spherical type models, which allows explaining a high degree of spatial dependence and a spatial behavior with associated and related aggregation centers. The populations of these problems were discovered to be closely related to one another, indicating that one is biologically dependent on the other. This will allow producers in this sector to manage their operations more effectively, potentially reducing chemicals, costs, and environmental impact in the region.

REFERENCES

Bautista LG, Cardona JA, Soto A. 2013. Spatial distribution of *Collaria scenica* (Hemiptera: miridae) and *Hortensia similis* (Hemiptera: Cicadellidae) in Andean Valleys. Boletín Científico Centro de Museos Museo de Historia Natural 17 (2): 75–84.

Cárdenas-Murillo R, Posada-Florez FJ. 2001. Los insectos y otros habitantes de cafetales y platanales. Centro Nacional de Investigaciones de Café: Chinchiná, Colombia. 250 p.

CEDRSSA (Centro de Estudios para el Desarrollo Rural Sustentable y la Soberanía Alimentaria). 2019. Investigación interna, comercio internacional, el caso de México. Ciudad de México, México. http://www.cedrssa.gob.mx/files/b/13/94Caf%C3%A9%20Producci%C3%B3n%20y%20Consumo.pdf (Retrieved: October 2022).

Esquivel-Higuera V, Jasso-García Y. 2014. Distribución espacial y mapeo de gusano soldado en seis localidades del Estado de México, en el año 2011. Revista Mexicana de Ciencias Agrícolas 5 (6): 923–935. https://doi.org/10.29312/remexca.v5i6.879

Fernandes FL, Picanço MC, Gontijo PC, de Sena Fernandes ME, Pereira EJG, Semeão AA. 2011. Induced responses of *Coffea arabica* to attack of *Coccus viridis* stimulate locomotion of the herbivore. Entomologia Experimentalis et Aplicatta 139: 120–127. https://doi.org/10.1111/j.1570-7458.2011.01113.x

Gil-Palacio Z. 2020. Servicios ecosistémicos en el cultivo del café. *In* Benavides-Machado P, Góngora CE. (eds.), El Control Natural de Insectos en el Ecosistema Cafetero Colombiano. Cenicafé: Bogotá, Colombia, pp: 186–203. http://doi.org/10.38141/10791/0001_8

Gómez-Campo K, Rueda M, García-Valencia C. 2010. Distribución espacial, abundancia y relación con características del hábitat del caracol pala *Eustrombus gigas* (Linnaeus) (Mollusca: Strombidae) en el archipiélago Nuestra Señora del Rosario, caribe colombiano. Boletín de Investigaciones Marinas y Costeras 39 (1): 137–159. http://doi.org/10.25268/bimc.invemar.2010.39.1.146

González-Vega ME, Hernández-Rodríguez A, Barrios-Alonso LM, Velázquez-del Valle MG, Hernández-Lauzardo AN. 2007. Efecto antagónico de un producto biológico obtenido de *Burkholderia cepacia* Palleroni & Holmes Contra *Capnodium* spp. en plántulas de café (*Coffea canephora* P.) crecidas *in vitro* e *in vivo*. Revista Mexicana de Fitopatología 25 (2): 120–126.

Jiménez-Carrillo R, Ramírez-Dávila J, Sánchez-Pale J, Salgado-Siclán M, Laguna CA. 2013. Modelización espacial de *Frankiniella occidentalis* (Thysanoptera: Thripidae) en tomate de cáscara por medio de técnicas geoestadísticas. Revista Colombiana de Entomología 39 (2): 183–192. https://doi.org/10.25100/socolen.v39i2.8232

Martínez-Martínez N, Ramírez-Dávila JF, Mejía-Carranza J, Vera-Noguez S. 2021. Comportamiento espacial de *Hemiberlesia lataniae* (Signoret) en aguacate "Hass" en el Estado de México. Ingeniería Agrícola y Biosistemas 13 (1): 33–52. https://doi.org./10.5154/r.inagbi.2021.01.005

Martínez-Ortega R, Tuya-Pendás L, Martínez-Ortega M, Pérez-Abreu A, Cánovas A. 2009. El coeficiente de correlación de los rangos de Spearman: caracterización. Revista Habanera de Ciencias Médicas 8 (2): 1–19.

Moral-García F. 2004. Aplicación de la geoestadística en las ciencias ambientales: Ecosistemas 13 (1): 78–86.

Oliver M, Webster R. 1998. How geostatistics can help you. Soil Use and Management 7 (4): 206–217. https://doi.org/10.1111/j.1475-2743.1991.tb00876.x

Ong WT, Vandermeer HJ. 2014. Antagonism between two natural enemies improves biological control of a coffee pest: The importance of dominance hierarches. Biological Control 76: 107–113. https://doi.org/10.1016/j.biocontrol.2014.06.002

Quiñones-Valdez R, Sánchez-Pale JR, Pedraza-Esquivel A, Catañeda-Vildozola A, Gutiérrez-Ibañez AT, Ramírez-Dávila JF. 2015. Análisis espacial de *Thrips* spp. (Thysanoptera) en el cultivo de gladiolo en la región sureste del Estado de México, México. Southwestern Entomologist 40 (2): 397–408. https://doi.org/10.3958/059.040.0213

Ramírez-Dávila JF. 2012. Geoestadística, principios básicos, aplicaciones y limitaciones. Universidad Autónoma del Estado de México: Toluca, México. 135 p.

Rivera-Martínez R, Ramírez-Dávila JF, Martínez-Quiroz M, González-Huerta A. 2020. Spatial modeling of *Bactericera cockerelli* Sulc nymphs on husk tomato (*Physalis ixocarpa* Brot.) using of geostatistical techniques. Biotecnia 22 (1): 142–152. https://doi.org/10.18633/biotecnia.v22i1.1162

Rivera-Martínez R, Ramírez-Dávila JF, Tapia-Rodríguez A, Figueroa-Figueroa DK, Acosta-Guadarrama A, Serrato-Cuevas R. 2022. Comportamiento espacial del barrenador de la rama en aguacate utilizando el método del SADIE en el Estado de México. Revista Mexicana de Ciencias Agrícolas 13 (2): 247–259. https://doi.org/10.29312/remexca.v13i2.2728

Schotzko DJ, O'keeffe LE. 1989. Geostatistical description of the distribution of *Lygus hesperus* (Heteroptera: Miridae) in lentils. Journal of Economic Entomology 82 (5): 1277–1288. https://doi.org/10.1093/jee/82.5.1277

SIAP (Servicio de Información Agroalimentaria y Pesquera). 2021. Producción Agrícola. Servicio de Información Agroalimentaria y Pesquera. http://www.siap.gob.mx/ (Retrieved: October 2022)

Solares-Alonso V, Ramírez-Dávila JF, Sánchez-Pale JR. 2011. Distribución espacial de trips (Insecta: Thysanoptera) en el cultivo de aguacate (*Persea americana* Mill.). Boletín del Museo de Entomología de la Universidad del Valle 12 (2): 1–12.

Tapia-Rodríguez A, Ramírez-Dávila JF, Salgado-Siclan M, Castañeda-Vildozola A, Maldonado-Zamora FI, Lara-Díaz AV. 2020. Distribución espacial de antracnosis (*Colletotrichum gloeosporoides* Penz) en aguacate en el Estado de México. Revista Argentina de Microbiología 52 (1): 72–81. https://doi.org/10.1016/j.ram.2019.07.004